

Oxygen Evolution Nickel Hydroxide Electrodes in a Ni-MH Battery Prototype

M.D. Becker¹, D.J. Cuscuela², H.R. Salva², F. Rodriguez Nieto³, A.A. Ghilarducci² and A. Visintin¹

¹INIFTA-CONICET, Diag. 113 y 64, 1900, La Plata, Argentina

²Centro Atómico Bariloche-CNEA, Instituto Balseiro-UNCuyo, CONICET, Av. Bustillo 9500, 8400, San Carlos de Bariloche, Argentina

³INIFTA-CIC, Diag. 113 y 64, 1900, La Plata, Argentina

Received: December 20, 2011, Accepted: February 10, 2012, Available online: May 22, 2012

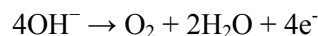
Abstract: The effect of cobalt in both alpha and beta phases on the oxygen evolution of nickel hydroxide was studied. The electrochemical properties of the oxygen evolution reaction on the positive nickel hydroxide electrodes were studied under conditions similar to those of a commercial Ni-MH battery. The presence of different kinds of defects in the structure of the active material was determined by XRD methods distorted and asymmetric reflections in the XRD patterns. Both the morphology of the active material and the additives influence the oxygen evolution potential and the electrochemical characteristics. The experimental results showed that the optimized prototype used in this work is suitable for evaluating several electrochemical parameters. It was shown that the electrode without cobalt exhibited the charging efficiency was 94% and those with cobalt exhibited a charging of 98%.

Keywords:

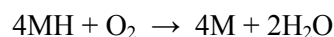
1. INTRODUCTION

Secondary batteries such as Ni-MH, Ni-Cd, Ni-H₂ have been used since the beginning of the twentieth century and at present they are widely used in batteries for portable devices such as those for aircraft and space application or in electric vehicles. In this kind of battery, nickel hydroxide is used as the positive electrode material [1,2]. Oxygen evolution is one of the most important factors influencing the quality of the battery because it is a parasitic reaction in the nickel hydroxide redox reaction during charging of nickel hydroxide electrodes, and oxygen gas bubble formation may contribute to electrode degradation by generating internal stresses within the electrode.

At high anode potential, oxygen gas evolves according to

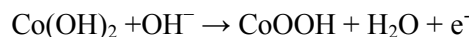


The oxygen evolved diffuses through the separator and reacts with the hydrogen stored in the negative electrode, causing the self-discharge as



The use of additives such as cobalt allows the increase of oxy-

gen overpotential and also the conductivity of active material [3,4], improving the charging efficiency. In terms of phases of nickel hydroxide, the alpha phase retards the overpotential because of the higher conductivity. In many works the influence of active material over oxygen evolution has been studied using a three-compartment electrolytic cell [5,6]. In this work the effect of cobalt in the alpha and beta phases of polymorphous nickel hydroxide was studied by analyzing the oxygen evolution during charge using a prototype Ni-MH cell. This kind of cell allowed us to follow oxygen evolution through the inner pressure. In the electrodeposition method Co(OH)₂ is coprecipitated with Ni(OH)₂ in the sintered Ni collector. The first charge transforms to CoOOH, which cannot be reduced during the subsequent discharging process, corresponding to the reaction



The addition of CoOOH provides a good electrical contact between the active material and the substrate and improves the utilization of the active material. The oxygen evolution overpotential increases and the oxygen evolution reaction is inhibited at the nickel hydroxide electrode coprecipitated with cobalt.

The nickel hydroxide coated with 5-10 wt % cobalt (III) oxide hydroxides considerably improves the utilization of active materi-

*To whom correspondence should be addressed: Email: dbecker@inifta.unlp.edu.ar

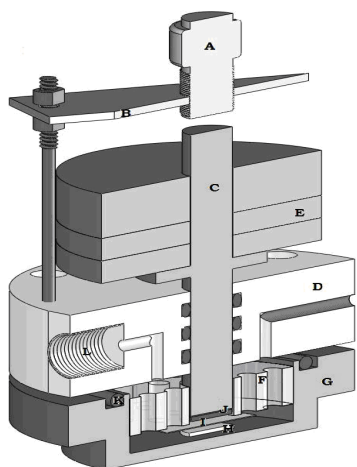


Figure 1. Cross-section of the battery prototype

als, discharge potential, rate-capacity properties, and cycling durability [7].

In this work the NiCo-EDH and NiCo-EDB electrodes have 10 wt % cobalt.

Charge/discharge experiments were carried out using α or β Ni(OH)₂ and NiCo-EDH and NiCo-EDB with approximately 10 wt % cobalt samples synthesized in our laboratory, coupled with a metal hydride (La_{0.95}Ni_{3.8}Co_{0.3}Mn_{0.3}Al_{0.4}) electrode. Both electrodes were protected by a separator simulating the conditions of a commercial battery with a prototype [8], which was adapted to a pressure transducer to measure the release of gases. The material of the prototype was properly selected considering a highly corrosive environment.

2. EXPERIMENTAL DETAILS

2.1. Prototype

The requirements for the design of the device should enable us to characterize the features of a commercial battery, such as limited physical space, electrical contact resistance, and system behavior as a function of gas evolution during charge and overcharge. Electrochemical characterization was performed using laboratory equipment.

Figure 1 shows the device used as battery container. It consists of a stainless steel main body where the electrodes, the separator and the electrolyte are placed. The metallic composition of the body and the top piston assure the electrical contact with the battery electrodes.

The device is composed of lock screw (A), guide for the piston (B), metallic piston (C), nylon top (D), masses for electrode compaction (E), nylon piece for electrode centering (F), metallic base (G), positive electrode (H), separator (I), negative electrode (J), O-ring (K) and duct for pressure transducer (L).

The evolution of gas was measured with a Siemens pressure transducer, working from vacuum to 600 kPa.

2.2. Negative electrode

The hydride-forming electrode (LmNi_{3.4}Co_{0.3}Mn_{0.3}Al_{0.8}) was prepared with 100 mg of Lm-based alloy powder mixed with an

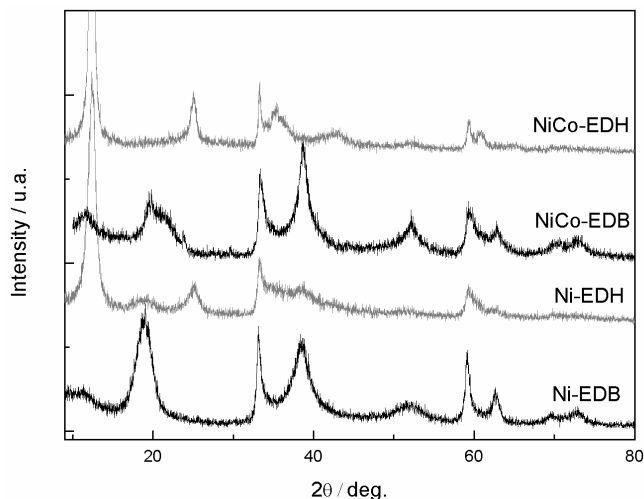


Figure 2. Powder XRD pattern of nickel hydroxide samples obtained by indirect chemical precipitation.

equal amount of teflonized carbon black (Vulcan XC-72 with 33 wt% PTFE) as mechanical support, and the mixture was then pressed into a cylindrical matrix under a pressure of 300 MPa at room temperature. The geometric area of the negative electrode was 78.5 mm² and the thickness was around 1.7 mm, with a storage capacity 50% higher than the discharge capacity of the positive electrode, so this electrode limits the capacity of the battery.

2.3. Positive electrode

Nickel and cobalt hydroxide powders containing approximately 10 wt% of cobalt hydroxide were obtained by indirect chemical precipitation using high area platinum as the cathode and sintered nickel plates of about 80% porosity as the anode of the electrochemical cell. The electrolysis was performed at high current density (\cong 1Amp) at 70°C and atmospheric pressure. X-Ray Diffraction (XRD) was used to study the phase composition of the prepared samples. Cobalt content was determined by atomic absorption spectroscopy.

2.4. Separator

A glass-based material was used as battery separator. The thickness of the glass woven roving material is 150 μ m and the area of the samples was large enough to avoid contact between the electrodes. The structure of the separator also ensures the permeability of the electrolyte.

2.5. Electrochemical characterization

The electrochemical performance of the battery was studied by charge-discharge cycles at constant current using homemade cycling galvanostat/potentiostat equipment considering that oxygen evolution occurs mainly during charge. Furthermore, the charge current was varied.

The sequence is described below:

- 5 cycles with charge current of C_n for 1.5 h and C_n discharge current and cutoff condition 0.8 V.
- 5 cycles with charge current of $1.5C_n$ for 1 h and discharge current and cutoff condition 0.8 V.

where C_n is the discharge capacity of the electrode when the discharge current is 149 mA/h/g.

3. RESULTS AND DISCUSSION

3.1. Positive electrode

For the XRD analysis, the sample was scanned from 10° to 80° (2θ) in steps of 0.02° . Figure 2 shows the XRD patterns. Ni-EDH and NiCo-EDH samples correspond to the α phase, while Ni-EDB and NiCo-EDB to the β phase. The patterns in Figure 2 do not show the cobalt lines, and the most important reflections of nickel hydroxide appear distorted and asymmetric, indicating the presence of a defective or amorphous structure. Table 1 lists some characteristics of the samples. From the Bragg peak broadening and using the Scherrer formula [9] it is possible to determine the crystal size within the basal plane (100) or perpendicular to the basal plane (001).

3.2. Cobalt influence

Figure 3 shows the oxygen pressure evolution curves as a function of percent of the *state of charge* (SOC) for the Ni-EDH and NiCo-EDH samples, corresponding to the alpha phase of nickel hydroxide with and without cobalt for the charge current rate $I_c = C_n$ (Figure 3a) and for $I_c = 1.5 C_n$ (Figure 3b). The results obtained show the clear effect of cobalt addition to the nickel hydroxide structure on the oxygen evolution reaction in alkaline solution. For the NiCo-EDH sample oxygen pressure evolution starts when the ca. 60% of the SOC is reached; whereas for Ni-EDH the oxygen pressure evolution starts at ca. 55% of the SOC. A similar behavior is observed when the charge current is increased, although in this case the SOC percent when oxygen pressure evolution starts is lower.

When the charge current is higher (Figure 3b), oxygen evolution starts before 100% of SOC in both electrodes, but electrodes with Co addition are still better than those without it.

Cobalt has an important influence over active material performance, such as: (1) an enhancement of the nickel electrode conductivity [10,11], (2) better chargeability by raising the oxygen overpotential and/or lowering the working electrode potential [12,13], (3) a minimization of γ -NiOOH growth at the nickel electrode during charging [14], and (4) an increase in the nickel electrode mechanical resistance [15-17]. Nevertheless, the principal advantage is the decrease in the difference between the oxidation and reduction peak potentials and a better charge/discharge behavior. Therefore the presence of cobalt in the active material delayed the oxygen evolution reaction (OER) and reduced Dp at the end of charge.

3.3. Structural influences

In the reduced state of Ni(OH)₂ there are two phases, β -Ni(OH)₂

Table 1. Characteristics of active materials of Ni(OH)₂

Samples	Co (%w/w)	Phase	FWHM (10l) $l \neq 0$ (2 θ)	Crystal size (nm)
Ni-EDB	0	β	1.85	14.6
Ni-EDH	0	α	1.04	13.0
NiCo-EDB	6.56	β	2.05	11.0
NiCo-EDH	8.80	α	2.76	17.2

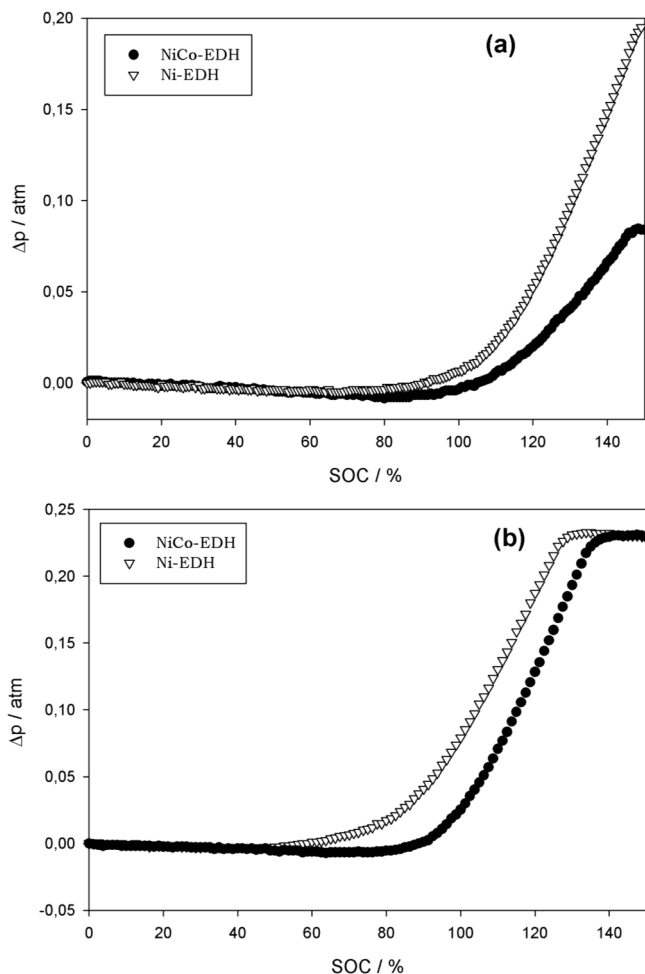


Figure 3. Pressure evolution during charge at the same state of recharges (a) $I_c = C_n$ and (b) $I_c = 1.5 C_n$

and α -Ni(OH)₂, that transform to β -NiOOH and γ -NiOOH during charging, respectively. In the active material, not only the purity or the mixture of phases is important but also the type of defects in the lattice structure. Figure 2 presents the powder XRD patterns of samples. The XRD patterns of the four samples prepared indicate the presence of particles in the form of β -Ni(OH)₂ and α -Ni(OH)₂, when compared with those of the standard pattern (JCPDS card No. 14-0117 and 00-022-0444), but the width of the peaks is different. Peak broadening in Ni(OH)₂ XRD patterns has often been correlated with electrochemical activity of the compound. Previous reports have indicated that peaks (001) and (10l) were especially broad when the nickel hydroxide was more active [18, 19].

From a general point of view three main types of stacking following a stacking fault were considered: (i) in the 'growth fault' the structure continues to grow with its natural packing rule, (ii) in the 'deformation fault' a part of the structure is displaced, and (iii) in the 'layer displacement fault' only one layer is modified in the part of the crystal considered [20-25]; all of them improve electrochemical performance [26]. This defect can be determined with full width at half maximum (FWHM) of line 10l ($l \neq 0$), where the broader the peak is, the higher the structural disorder results.

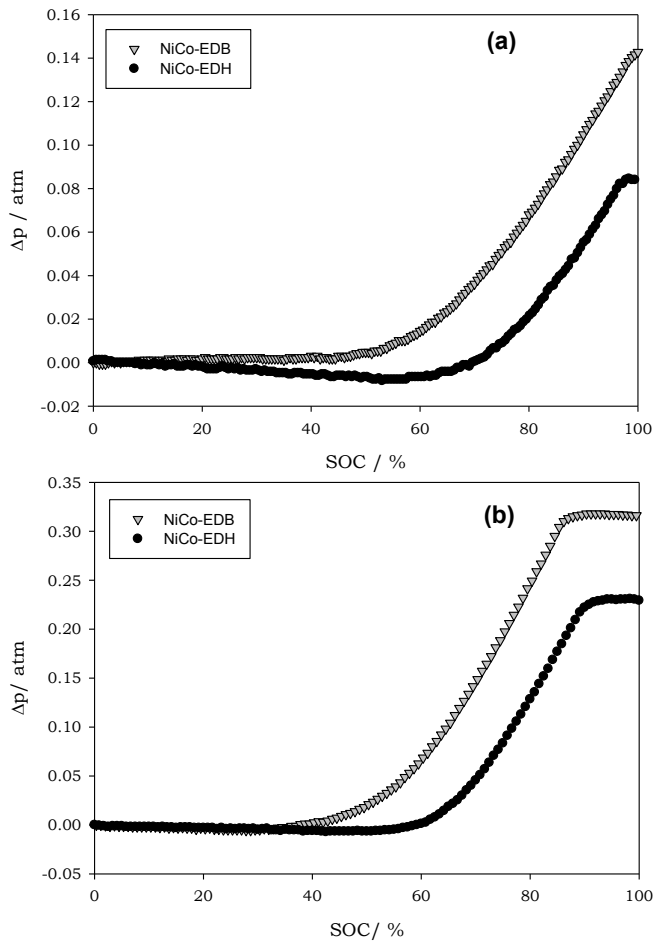


Figure 4. Pressure evolution during charge at the same state of recharges (a) $I_c=C$ and (b) $I_c=1.5C$

If we compare electrodes that were built with the same content of cobalt but a different structure of nickel hydroxide, we can see that α -Ni(OH)₂ (NiCo-EDH) further delays oxygen evolution, achieving a better charging efficiency than the β -Ni(OH)₂ (NiCo-EDB) electrode (Figure 4).

The electrode built with α -nickel hydroxide (NiCo-EDH) shows less increase of pressure during charge than an electrode that was built with β -nickel hydroxide (NiCo-EDB). At high rate current the profile has the same behavior as at low rate current. This behavior is directly related to the active material conductivity [25].

Figures 5 and 6 show different sizes and shapes of particles that are part of the active material. In the SEM micrograph of sample NiCo-EDB (Figure 5) particles show well-defined facets indicating some crystallinity and are larger than the particles of NiCo-EDH (Figure 6), which are amorphous and smaller. So the electrode built with material of smaller particle size will have a higher active area, suggesting that the charge-discharge process is more reversible and the oxygen evolution potential is more positive [26].

3.4. Charging efficiency

The prototype designed permits the measurement of the total charge (q_{total}) during the experiment that involves the charge for

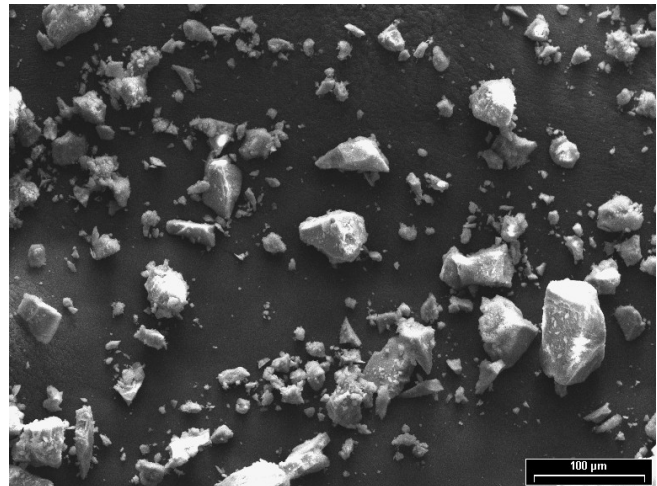


Figure 5. Micrograph of NiCo-EDB

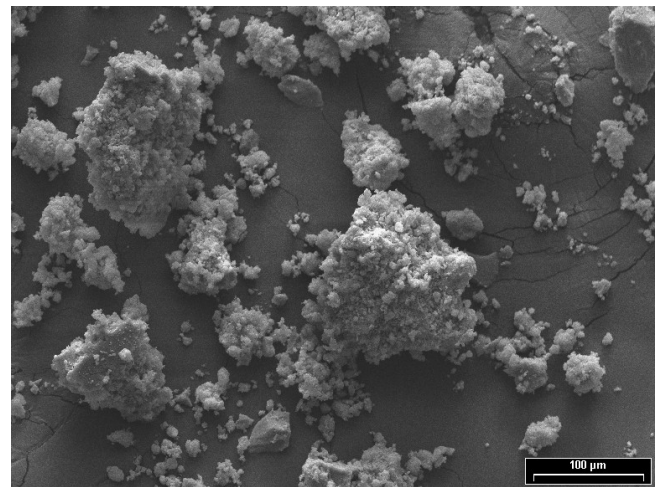
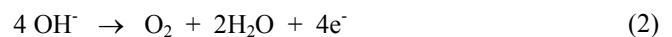


Figure 6. Micrograph of NiCo-EDH

Ni⁺² to Ni⁺³ transformations ($q_{\text{Ni}^{+2}/\text{Ni}^{+3}}$) and the charge for oxygen evolution from the electrolysis of aqueous solution. It is possible to distinguish between the two charges and calculate the charging efficiency ($\%Ef_{\text{charge}}$) using Faraday's laws

$$\%Ef_{\text{charge}} = 100 \times \frac{q_{\text{Ni}^{+2}/\text{Ni}^{+3}}}{q_{\text{total}}} \quad (1)$$

Considering the OER in an aqueous alkaline medium



and assuming an ideal gas behavior, the inside pressure (P_{in}) is the addition of oxygen pressure (P_{O_2}) and vapor pressure of water ($P_{\text{H}_2\text{O}}$)

$$P_{\text{in}} = P_{\text{H}_2\text{O}} + P_{\text{O}_2} \quad (3)$$

where P_{in} was measured with the transducer and $P_{\text{H}_2\text{O}}$ is $P_{\text{H}_2\text{O}} = 23.746 \text{ mmHg}$ at 25 °C

P_{O_2} is the difference between P_{in} and P_{H_2O}

$$P_{O_2} = P_{in} - P_{H_2O} \quad (4)$$

$$P_{O_2} = \frac{n_{O_2} \cdot R \cdot T}{V_v} \quad (5)$$

For the previous equation oxygen mole (n_{O_2}) is

$$\frac{P_{O_2} \cdot V_v}{R \cdot T} = n_{O_2} \quad (6)$$

where R is the ideal gas constant and V_v is the free volume inside the prototype

$$R = 0.082 \left[\frac{l \cdot atm}{mol \cdot K} \right]$$

The oxygen moles that were generated during the state of charge were obtained taking into account the electrochemical equivalent of oxygen (ξ)

$$\xi = 8 \left[\frac{gr_{O_2}}{C} \right]$$

$$\frac{n_{O_2} \cdot PM_{O_2}}{\xi} = q_{O_2} \quad (7)$$

where

$$q_{O_2} = I_{O_2} \cdot t \quad (8)$$

and

$$q_{total} - q_{O_2} = q_{Ni^{2+}/Ni^{3+}} = I_{Ni^{2+}/Ni^{3+}} \cdot t \quad (9)$$

where I_{O_2} is the current participating in oxygen evolution, $I_{Ni^{2+}/Ni^{3+}}$ is the current for Ni^{+2} to Ni^{+3} transformations and t is charge time.

It is possible to calculate the charge participating in oxygen evolution (q_{O_2}) and the transformation from Ni^{+2} to Ni^{+3} . Figures 7a and 7b show the current profiles that participated in the charge process. At the end of charge the energy stored is less than expected.

In the electrode without cobalt (Figure 7a) the charging efficiency was 94% and for the electrode containing cobalt (Figure 7b) the charging efficiency increased to 98%. This result indicates that cobalt increases the conductivity, oxygen evolution potential and active material utilization.

4. CONCLUSIONS

Based on the results obtained in this work it may concluded that:

i) XRD patterns present broader and asymmetric reflections, indicate that the nickel hydroxide samples prepared are highly defective and amorphous, and the presence of defects such as stacking fault in the lattice structure raises charging efficiency.

ii) The prototype developed in this work is suitable for measuring

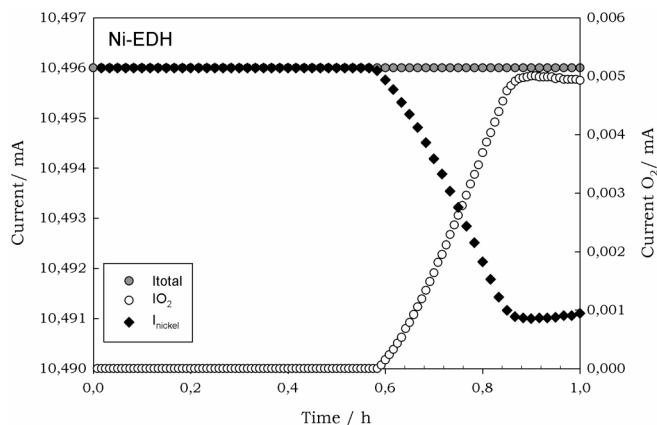


Figure 7a. Charge current variation (charge current= $1.5C_n$) as a function of time for the Ni-EDH electrode.

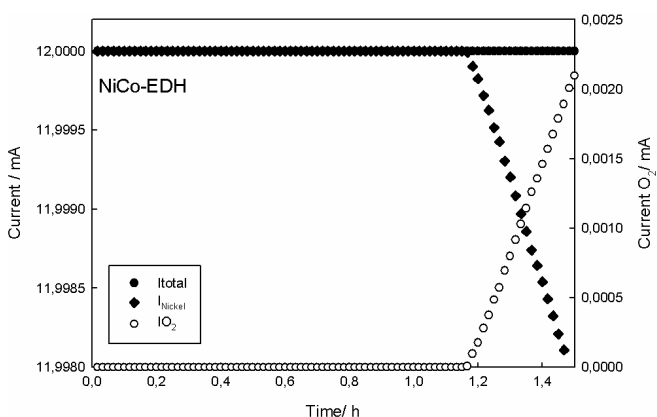


Figure 7b. Charge current variation (charge current= $1.5C_n$) as a function of time for the NiCo-EDH electrode.

different electrochemical parameters and especially for studying the oxygen evolution reaction.

iii) The experimental results showed that the presence of cobalt in the active material delays the oxygen evolution reaction and decreases overpressure during the state of charge. Moreover the alpha nickel hydroxide structures present a better electrochemical performance.

iv) The electrode without cobalt exhibited the charging efficiency was 94% and those with cobalt exhibited a charging of 98%.

5. REFERENCES

- [1] D.A. Corrigan and R.M. Bendert, J. Electrochem. Soc., 136, 723 (1989).
- [2] R.M. Barnard, C.F. Randell, F.L. Tye, J. Appl. Electrochem., 10, 127 (1980).
- [3] C. Faure, C. Delmas, P. Willmann, J. Power Sources, 36, 497 (1991).
- [4] J.Y. Xie, Q.S. Zhang, J.F. Liu, P.F. Shi., Chin J. Power Sources, 23, 238 (1999).
- [5] J.Y. Xie, Q.S. Zhang, J.F. Liu, P.F. Shi, Chin. J. Power Sources,

- 23, 22 (1999).
- [6] L. Demourgues-Guerlou, L. Faure, C. Delmas, J. Electrochem Soc., 143, 561(1996).
- [7] J. Li, L. Rong, J.M. Wu, S. Hang, J. Power Sources, 79, 86 (1999).
- [8] D.J. Cuscueta, PhD thesis, 2010.
- [9] A. Patterson, Phys. Rev. 56, 10, 978 (1939).
- [10] M. Oshitani, H. Yufu, K. Takashima, S. Tsuji and Y. Massumaru, J. Electrochem. Soc., 136 (1989).
- [11] L. Gautier, Thesis, University of Bordeaux I, 1995.
- [12] B.E. Ezhov and O.G. Malandrin, J. Electrochem Soc, 138, 885 (1991).
- [13] R.D. Armstrong and E.A. Charles, J. Power Sources, 25, 89 (1989).
- [14] J. Mc Breen, W.E. O'Grady, G. Tourillon, E. Dartyge, A. Fontaine and K.I. Pandya, J. Phys. Chem., 93, 6308 (1989).
- [15] R.D. Armstrong, G.W.D. Briggs and E.A. Charles, J. Appl. Electrochem., (1988).
- [16] H. Chen, J.M. Wang, T. Pan, Y.L. Zhao, J.Q. Zhang, C.N. Cao, J. Power Sources, 143, 243 (2005).
- [17] X.Y. Wang, H. Luo, H.P. Yang, P.J. Sebastian, S.A. Gamboa, Int. J. Hydrogen Energy, 29, 967 (2004).
- [18] C. Delmas, C. Tessier, J. Mater. Chem., 7, 1439 (1997).
- [19] M.C. Bernard, R. Cortes, M. Keddad, H. Takenouti, P. Bernard, S. Senyarich, J. of Power Sources, 63, 247 (1996).
- [20] A.A. Kamnev, Electrochim. Acta, 41, 267 (1996).
- [21] L. Indira, M. Dixit, P.V. Kamata, Journal of Power Sources 52, 93 (1994).
- [22] X.X. Yuan, Y.D. Wang, F. Zhang, J. Mater. Sci. Technol. 17, S119 (2001).
- [23] M. Oshitani, M. Watada, K. Shodai, M. Kodama, J. Electrochem. Soc. 148 A67 (2001).
- [24] R. Barnard, C. Randell, and F.L. Tye, Power Sources, Academic Press, London 8, 401 (1981).
- [25] C. Tessier, P.H. Haumesser, P. Bernard, and C. Delmas, J. Electrochem. Soc. 146, 2059 (1999).
- [26] A.M. Bond, S. Fletcher, P.G. Symons, Analyst 123, 1891 (1998).